MINIATURE SPECTROMETER FOR DETECTION OF ORGANICS AND IDENTIFICATION OF THEIR MINERAL CONTEXT. Nancy J. Chanover[1], David A. Glenar[1], Kyle Uckert[1], David G. Voelz[1], Xifeng Xiao[1], Rula Tawalbeh[1], Penelope Boston[2], William Brinckerhoff[3], Stephanie Getty[3], and Paul Mahaffy[3] [1]New Mexico State University, Las Cruces, NM, USA, [2]New Mexico Institute of Mining and Technology, Socorro, NM USA, [3]NASA/Goddard Space Flight Center, Greenbelt, MD, USA

Introduction: On future landed missions to Mars and small solar system bodies, efficient sample prescreening will be necessary to select interesting targets for further analysis by analytical instruments with very limited time and power resources. Near infrared spectroscopy is well suited for rapid and non-invasive identification of mineral classes, and the possible presence of organic molecules. A small spectrometer on the surface also enables ground-truth for orbiting reflectance spectrometers operating at overlapping wavelengths [1, 2]. Here we describe a miniature acousto-optic tunable filter (AOTF) point spectrometer that is tunable from ~1.6 - 3.6 μm. It identifies minerals associated with aqueous environments at sample scales of ~ 1 mm, as well as organic molecules and volatiles (notably H_2O and CO_2 ice), where they are present.

AOTFs have previously been used on board Mars Express [3] and Venus Express [4] as integral components of their IR spectrometers. They are inherently rugged, radiation-hard, rapidly tunable and can operate at cryogenic temperatures, so they are a suitable choice for miniature landed-spectrometers. Our group also has a demonstrated history of developing and using AOTF devices for planetary science imaging applications [5-10].

Our new point spectrometer can be combined with other diagnostic instruments as part of a landed instrument package. It is presently being integrated with a laser-desorption time-of-flight mass spectrometer LDTOF developed at GSFC, and will prescreen samples for evidence of organics before the laser desorption step and subsequent mass spectrometer measurement. The addition of AOTF technology has the potential to enable significant near-IR spectroscopic diagnostic capability without exceeding the resources of a small surface laboratory.

Design and Operation: A schematic of the point spectrometer optics (Fig. 1) shows its operation at a conceptual level. The spectrometer can be divided into source and detector subsections.

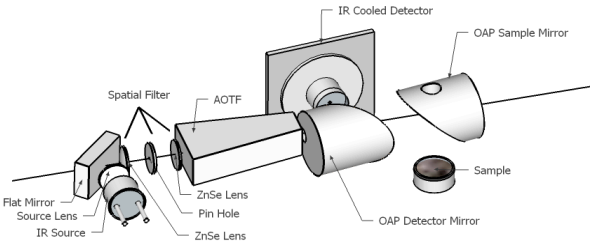

Figure 1. 3D layout showing the spectrometer optics.

Light Source Optics: The source itself is a miniature tungsten IR lamp (effective temperature ~1900 K) with sapphire windows. Broadband lamp light is reimaged onto a 1 mm field stop to reject out-of-field rays, and then recollimated using anti-reflection coated ZnSe lenses. The tuning element is a TeO_2 AOTF crystal, which transmits a narrow spectral slice, with peak transmittance of ~30-70%, depending on wavelength (only one linear polarization is transmitted). The wavelength of the output light is determined by the RF frequency applied to a transducer bonded to the AOTF. The spectral coverage of the AOTF-detector combination is ~1.6–3.6 μm, requiring a frequency range for the RF drive signal of 29–70 MHz at the long and short wavelength limits, respectively, and drive power of 2-3 W. Spectral resolution ($R = \lambda/\Delta\lambda$) is wavelength dependent and ranges from ~200 to more than 400 over the wavelength tuning range, with highest resolution at the shortest wavelengths.

Detector Optics: The sample illumination and detector optics serve as a biconical reflectance spectrometer with small (~f/4) and large (~f/1) solid angles for source and reflected beams, respectively. It consists of sample surface, two 25 mm, 90 degree, off-axis parabolic mirrors that collect the scattered light and reimage it at 1:1 magnification onto a thermoelectrically cooled (-65°C) MCT detector. Narrow-band source light is imaged by the sample mirror onto a small (< 2 mm diameter) spot on the sample surface. Reflected light then fills the aperture of the sample mirror, which reimages the illuminated sample spot on the detector. The point spectrometer is depicted in Fig. 2, and Table 1 lists the instrument specifications.

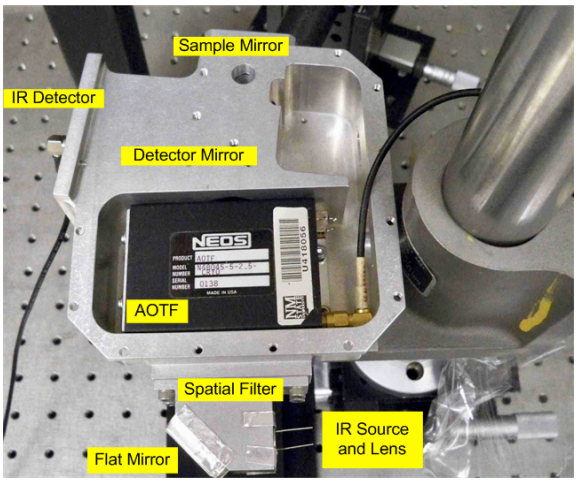

Figure 2. Photo showing the point spectrometer during initial tests. The main components are labeled.

Data Acquisition: A geologic sample is placed at the focus point of the spectrometer, approximately 2 cm below the optical centerline. The RF signal is pulsed through the AOTF crystal over the entire 29-70 MHz frequency range, as light covering a narrow wavelength range falls on the detector. The RF frequency is set to 0 MHz at regular intervals throughout the data acquisition process to allow broadband light through the crystal to calibrate the signal. Measurements of an infragold plate, a Lambertian reflector whose reflectivity is uniform over the entire wavelength range, are also taken as a reference spectrum. A tuning curve was developed to define the wavelength scale of the AOTF by placing narrow-band IR filters in the optical path during measurements of an infragold sample.

Table 1. Spectrometer Specifications

Wavelength Coverage (μm):	1.6 – 3.6
RF Tunable	29 – 70 MHz
Spectral Resolution (nm):	4 - 12
Sample field-of-view (mm):	1.5
Full-on power requirements (W), AOTF	2-3
IR Lamp	2
TE cooler	3
Spectrometer fixture, mass (kg):	1.5
Vol (cm^3):	630

Spectral Survey of Aqueous Minerals: Spectral detection of organic molecules on mineral surfaces first requires a thorough characterization of the uninhabited host minerals, measured using the same instrument. We routinely acquire near-IR spectra of field samples including evaporites (sulfates, carbonates), clays, and oxides, all of which can be linked to aqueous environments and are therefore of high astrobiological interest.

Sulfates: In the case of gypsum, sulfate ($-SO_4$) bands are directly observed only at longer wavelengths, but distinctive bound water features do appear at numerous wavelengths. Most diagnostic of gypsum at these wavelengths is the blended feature with reflectance minimum at ~1.9 μm. All of these features are much weaker (or disappear entirely) in the anhydrous form (anhydrite, $CaSO_4$). The solid line in Fig. 3(a) shows the spectrum of potassium jarosite ($KFe_3(OH)_6(SO_4)_2$). The dominant feature is the strong cluster of Fe-OH features with reflectance minimum at 2.27 μm [11, 12].

Carbonates: The sequence of bands that appear in Fig. 3(b) are combination and overtone bands of the carbonate ion, and their sequence and prominence are indicative of carbonates. As noted by [13], the wavelengths of the band reflectance minima depend on the metal cation. As shown in Fig. 3(b), the positions of these bands in dolomite ($CaMg(CO_3)_2$) lie at systematically shorter wavelengths than that of calcite ($CaCO_3$), which allows these carbonates to be uniquely identified if spectral resolution and signal-to-noise ratio are sufficient.

Clays: Both the Kaolinite and Montmorillonite (Bentonite) spectra in Fig. 3(c) show familiar clay absorption features near 1.9 and 2.2 μm, and a pronounced OH stretching vibration near 2.75 μm. Strong features near 2.2 μm are metal-OH combination bands [14]. The shape, depth and minimum reflectance wavelength of these features depends on composition. In the case of Kaolinite ($Al_2Si_2O_5(OH)_4$), the feature is an Al-OH combination band that appears as a distinctive doublet. The 1.9 μm feature is an OH-stretch, H_2O-bend combination band that requires both H_2O and OH to be present [15]. As shown by [16], the depth of this feature is dramatically reduced under low pressure-temperature conditions, which simulate the Mars environment.

Iron Oxides: Although our focus is evaporites and clays, we also included iron oxides, as shown in Fig. 3(d), since they are ubiquitous in Martian soils. Most spectral features distinctive of iron oxides or oxy-hydroxides are found at shorter wavelengths (e.g. the steep UV-visible red slope due to the Fe^{3+} cation). Within our wavelength coverage, Hematite (α-Fe_2O_3) is mostly featureless except for the 3 μm bound water absorption. On the other hand, the hydrated form, Goethite (α-FeO(OH)), shows broad infrared absorptions near 1.9 and 2.4 μm (see Fig. 3(d)).

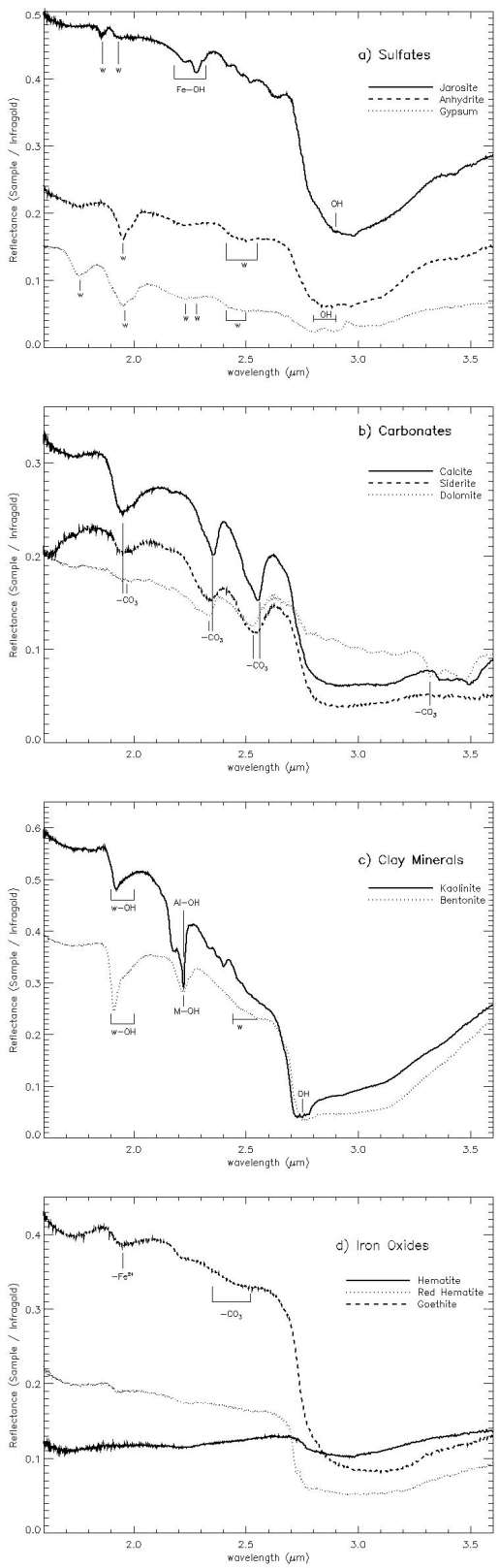

Figure 3. Spectral survey of field samples using the point spectrometer.

Identification of Organics: In addition to mineral standards, we examined mixtures of organic coatings on inorganic substrates. An example of an organically doped mineralogical sample is shown in Figure 4. Here, we added a 150 μL volume of Pyrene dissolved in dichloromethane at a concentration of 1 mg/ml to a rock chip of vesicular olivine basalt. The lower part of the figure shows the strong C-H stretching transitions, which lie in the region expected for aromatic hydrocarbons. This measurement included a possible error in the spectrometer wavelength calibration, and we have shifted the spectrum to coincide with the predicted band position.

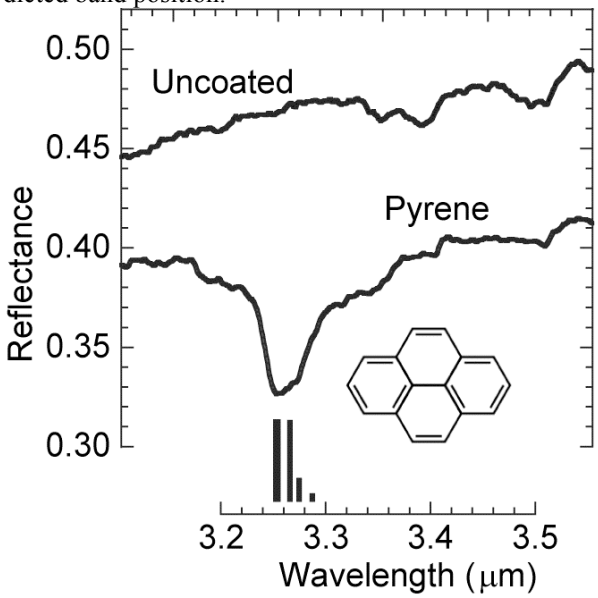

Figure 4. Spectrum of Pyrene coating on basalt chip, and comparison spectrum of an uncoated sample. The lower part of the plot shows one Pyrene structure, and the locations and relative intensities of the spectral transitions.

A Combined IR, Mass-Spectrometer Instrument Suite: The AOTF point spectrometer described herein is designed to be paired with a laser desorption time-of- flight (LDTOF) mass spectrometer, which provides pulsed-laser desorption and analysis of refractory organic compounds up to 150,000 Da on a spatial scale of 50-100 μm, determined by the laser spot size at the target. A geologic sample will be screened by the AOTF instrument to identify spectral features containing organic biomarkers or mineralogical signatures suggestive of extant or extinct life. If a sample of astrobiologic interest is identified, the LDTOF mass spectrometer is signaled to perform detailed follow-up observations to determine the elemental and organic constituents of the sample.

The recent integration of the two instruments allowed for coincident spectral measurements of a geologic sample. The LDTOF mass spectrometer shares an optical axis with the AOTF; follow-up measurements from the LDTOF are taken from an identical region on a sample of interest, allowing for a direct comparison between each complementary data set.

The AOTF could be deployed in a variety of configurations, either as a stand-alone instrument or paired with the LDTOF, depending on the nature of the mission. These include application as a contact sensor, such as on a robotic arm, or within an integrated "laboratory" payload on a lander or rover. The simplest implementation would entail operating the AOTF as a point spectrometer, with appropriate precision in relative positioning of the illumination/detector optics and the sample surface. By design, the AOTF and LDTOF spectrometers share a common working distance of several mm, and as such could alternatively be combined with a sample manipulation system that enables high-resolution dual-sensor chemical imaging. On an airless body such as a comet or icy satellite, this could be achieved without significant sample handling given the ambient high vacuum conditions. On Mars or Titan, there would need to be some level of sample manipulation to enclose and seal the sample.

This work was supported by grants from NASA's Experimental Program to Stimulate Competitive Research (EPSCoR) and Astrobiology Science and Technology Instrument Development (ASTID) programs, specifically through award numbers NNX08AY44G (ASTID) and NNX08A V85A (EPSCoR). Additional support was provided by New Mexico Tech, NMSU's Astronomy and Electrical and Computer Engineering Departments, the New Mexico EPSCoR program office, the NMSU Vice President for Research, and the NMSU ADVANCE Program.

References: [1] Murchie, S. L. *et al.* (2009) *JGR, 114*, E00D06, doi:10.1029/2009JE003342. [2] Bibring, J.-P. *et al.* (2005), *Science, 307,* 1576 – 1581. [3] Korablev, O. *et al.* (2006), *Geophys. Res. Let., 111*, E09S03, doi:10.1029/2006JE002696. [4] Bertaux, J.-L. *et al.* (2007), *Planet. Space Sci., 55*, 1673-1700. [5] Glenar, D. A. *et al.* (1994), *Appl. Optics, 33*, 7412-7424. [6] Glenar, D. A. *et al.* (1997), *Publ. Astron. Soc. Pacific, 109*, 326-337. [7] Glenar, D. A., Blaney, D. L. and Hillman, J. J. (2002), *Acta Astronautica, 1824*, 1-8. [8] Georgiev, G., Glenar, D. A. and Hillman, J. J. (2002), *Appl. Optics, 41*, 209-217. [9] Chanover, N. J. *et al.* (1998), *JGR, 103*, 31335-31348. [10] Chanover, N. J. *et al.* (2003), *Icarus, 163*, 150-163. [11] Frost, R. L. *et al.* (2005), *Spectrochimica Acta, 62*, 869-874. [12] Gilmore, M. S. *et al.* (2008), *Icarus, 195*, 169-183. [13] Gaffey, S. J. (1986), *American Mineralogist, 47*, 700-717. [14] Post, J. L. and Noble, P. N. (1993), *Clays and Clay Minerals, 41*, 639-644. [15] Clark, R. N. (1999), in *Manual of Remote Sensing, Volume 3, Remote Sensing for the Earth Sciences,* (A.N. Rencz, ed.), New York: John Wiley and Sons. [16] Bishop, J. L. *et al.* (1995), *Icarus, 117*, 101-119.